Supporting Information

Systematic study of a family of butterfly-like $\{M_2Ln_2\}$ molecular magnets (M = Mg^{II}, Mn^{III}, Co^{II}, Ni^{II} and Cu^{II}; Ln = Y^{III}, Gd^{III}, Tb^{III}, Dy^{III}, Ho^{III} and Er^{III})

Eufemio Moreno Pineda[§], *Nicholas F. Chilton, Floriana Tuna, Richard E. P. Winpenny* and Eric J. L. McInnes**

School of Chemistry and Photon Science Institute, The University of Manchester, Oxford Road, Manchester M13 9PL, United Kingdom. eric.mcinnes@manchester.ac.uk; Richard.Winpenny@manchester.ac.uk

§. Current address: Institute of Nanotechnology, Karlsruhe Institute of Technology, D-76344, Eggenstein-Leopoldshafen, Germany.

Synthesis of starting materials

Unless stated otherwise, all reagents and solvents were purchased from Aldrich Chemicals and used without further purification. $[M_2^{II}(\mu\text{-}OH_2)(O_2C^tBu)_4(HO_2C^tBu)_4]$ (M = Mg^{II}, Co^{II} and Ni^{II}), $[Mn_2^{II}(O_2C^tBu)_4EtOH]_n$ and $[Cu_2^{II}(O_2C^tBu)_4(HO_2C^tBu)_2]$ were prepared according to described procedures. $[Ln_2^{III}(O_2C^tBu)_6(HO_2C^tBu)_6]$ (Ln^{III} = Y, Gd, Tb, Dy, Ho and Er), were synthesised by refluxing $Ln^{III}{}_2O_3$ (10 mmol) and excess pivalic acid (30 g, 300 mmol) at 160 ºC for 5 hrs to form a clear solution. Followed by cooling the solution to room temperature and white or pink precipitate came out then 50 mL toluene was added to dissolve the access pivalic acid and filtered in vacuum and 50 ml *n*-hexane were used to wash the product (yield *ca*. 13 g, 87 %).

CASSCF method

CASSCF calculations were performed with MOLCAS 7.8. All calculations were on single isolated molecules, excluding counter-ions, and employed the experimental crystal structure with no optimization. Only one of the dysprosium sites was examined for each cluster, as the cluster possess inversion symmetry, therfore the other Dy^{III} site was replaced with Lu^{III}. For the cases with paramagnetic 3d ions, these were replaced by the diamagnetic analogues Zn^{II} (for Co^{II}, Ni^{II} and Cu^{II}) or Ga^{III} (for Mn^{III}). The basis sets were chosen from the ANO-RCC library, where the Dy ion was treated with VTZP quality, the first coordination sphere with VDZP quality, all other non-hydrogen atoms with VDZ quality and hydrogen atoms with MB quality. The two-electron integrals were Cholesky decomposed to reduce computational demands. In the RASSCF module, the sextets and

quartetes were state averaged with 21 and 224 roots, respectively. In the RASSI module, all 21 sextets and 128 quartets were mixed by spin-orbit coupling. No doublets were included in the calculation due to computational limitations.

Table S1. Elemental analysis and yield (%) for compounds **1** - **27**

	Formula	Yield[a] %	Elemental analysis: Found (calculated)				
			C	**H**	**N**	**M**	**Ln**
1	$[Mg^{II}_2Y^{III}_2(\mu\text{-}OH_3)(O_2C^tBu)_4(HO_2C^tBu)_4](^iPr_2NH_2)_2$	90	50.31 (50.45)	8.38 (8.47)	1.94 (1.90)	3.19 (3.29)	12.00 (12.05)
2	$[Mg^{II}_2Gd^{III}_2(\mu\text{-}OH_3)(O_2C^tBu)_4(HO_2C^tBu)_4](^iPr_2NH_2)_2\cdot$MeCN	79	45.56 (46.48)	7.82 (7.74)	2.84 (2.54)	2.92 (2.94)	19.08 (19.02)
3	$[Mg^{II}_2Tb^{III}_2(\mu\text{-}OH_3)(O_2C^tBu)_4(HO_2C^tBu)_4](^iPr_2NH_2)_2$	87	45.92 (46.08)	7.74 (7.73)	1.72 (1.73)	2.99 (3.00)	19.56 (19.67)
4	$[Mg^{II}_2Dy^{III}_2(\mu\text{-}OH_3)(O_2C^tBu)_4(HO_2C^tBu)_4](^iPr_2NH_2)_2$	92	45.86 (45.87)	7.83 (7.70)	1.69 (1.73)	2.98 (2.99)	20.03 (20.02)
5	$[Mg^{II}_2Ho^{III}_2(\mu\text{-}OH_3)(O_2C^tBu)_4(HO_2C^tBu)_4](^iPr_2NH_2)_2$	87	45.86 (45.74)	7.88 (7.68)	1.68 (1.72)	2.93 (2.99)	20.10 (20.26)
6	$[Mg^{II}_2Er^{III}_2(\mu\text{-}OH_3)(O_2C^tBu)_4(HO_2C^tBu)_4](^iPr_2NH_2)_2$	93	44.79 (45.61)	7.78 (7.66)	1.70 (1.72)	2.88 (2.98)	20.39 (20.49)
7	$[Mn^{III}_2Y^{III}_2(\mu\text{-}OH_3)(O_2C^tBu)_4(HO_2C^tBu)_4](Et_3N)_2\cdot$MeCN	48	48.86 (48.76)	8.06 (7.99)	2.74 (2.67)	7.05 (6.97)	11.32 (11.28)
8	$[Mn^{III}_2Gd^{III}_2(\mu\text{-}OH_3)(O_2C^tBu)_4(HO_2C^tBu)_4](Et_3N)_2$	44	44.64 (44.54)	7.26 (7.35)	1.64 (1.67)	6.56 (6.57)	18.64 (18.81)
9	$[Mn^{III}_2Tb^{III}_2(\mu\text{-}OH_3)(O_2C^tBu)_4(HO_2C^tBu)_4](Et_3N)_2\cdot$MeCN	30	44.86 (44.78)	7.31 (7.34)	2.47 (2.45)	6.28 (6.40)	18.42 (18.52)
10	$[Mn^{III}_2Dy^{III}_2(\mu\text{-}OH_3)(O_2C^tBu)_4(HO_2C^tBu)_4](Et_3N)_2\cdot$MeCN	74	44.55 (44.60)	7.27 (7.31)	2.65 (2.44)	6.32 (6.37)	18.73 (18.86)
11	$[Mn^{III}_2Ho^{III}_2(\mu\text{-}OH_3)(O_2C^tBu)_4(HO_2C^tBu)_4](Et_3N)_2\cdot$MeCN	36	44.34 (44.47)	7.40 (7.29)	2.65 (2.43)	6.54 (6.36)	19.11 (19.08)
12	$[Mn^{III}_2Er^{III}_2(\mu\text{-}OH_3)(O_2C^tBu)_4(HO_2C^tBu)_4](Et_3N)_2\cdot$MeCN	42	44.34 (44.35)	7.34 (7.27)	2.31 (2.42)	6.27 (6.34)	19.39 (19.30)
13	$[Co^{II}_2Y^{III}_2(\mu\text{-}OH_3)(O_2C^tBu)_4(HO_2C^tBu)_4](^iPr_2NH_2)_2$	76	48.27 (48.19)	8.08 (8.09)	1.87 (1.81)	7.62 (7.63)	11.58 (11.51)
14	$[Co^{II}_2Gd^{III}_2(\mu\text{-}OH_3)(O_2C^tBu)_4(HO_2C^tBu)_4](^iPr_2NH_2)_2\cdot$MeCN	63	44.38 (44.61)	7.58 (7.42)	2.40 (2.44)	6.74 (6.84)	18.36 (18.25)
15	$[Co^{II}_2Tb^{III}_2(\mu\text{-}OH_3)(O_2C^tBu)_4(HO_2C^tBu)_4](^iPr_2NH_2)_2$	35	43.90 (44.00)	7.41 (7.39)	1.76 (1.66)	6.83 (6.96)	19.24 (19.20)
16	$[Co^{II}_2Dy^{III}_2(\mu\text{-}OH_3)(O_2C^tBu)_4(HO_2C^tBu)_4](^iPr_2NH_2)_2$	75	44.30 (44.34)	7.54 (7.38)	2.30 (2.42)	6.92 (6.80)	18.62 (18.75)
17	$[Co^{II}_2Ho^{III}_2(\mu\text{-}OH_3)(O_2C^tBu)_4(HO_2C^tBu)_4](^iPr_2NH_2)_2$	34	43.70 (43.87)	7.56 (7.36)	1.56 (1.65)	6.90 (6.94)	19.36 (19.43)
18	$[Co^{II}_2Er^{III}_2(\mu\text{-}OH_3)(O_2C^tBu)_4(HO_2C^tBu)_4](^iPr_2NH_2)_2$	32	42.62 (43.75)	7.41 (7.34)	1.60 (1.65)	6.81 (6.92)	19.50 (19.65)

19	$[Ni^{II}_2Y^{III}_2(\mu\text{-}OH_3)(O_2C^tBu)_4(HO_2C^tBu)_4](Et_3NH)_2$	40	48.07 (48.20)	7.96 (8.09)	1.81 (1.81)	7.43 (7.60)	11.67 (11.51)
20	$[Ni^{II}_2Gd^{III}_2(\mu\text{-}OH_3)(O_2C^tBu)_4(HO_2C^tBu)_4](Et_3NH)_2$	45	44.48 (44.62)	7.43 (7.43)	2.34 (2.44)	6.53 (6.81)	18.25 (18.26)
21	$[Ni^{II}_2Tb^{III}_2(\mu\text{-}OH_3)(O_2C^tBu)_4(HO_2C^tBu)_4](Et_3NH)_2$	74	44.14 (44.20)	7.53 (7.42)	1.68 (1.66)	6.95 (6.97)	18.64 (18.86)
22	$[Ni^{II}_2Dy^{III}_2(\mu\text{-}OH_3)(O_2C^tBu)_4(HO_2C^tBu)_4](Et_3NH)_2$	55	43.91 (44.01)	7.41 (7.39)	1.63 (1.66)	6.82 (6.94)	19.30 (19.21)
23	$[Ni^{II}_2Ho^{III}_2(\mu\text{-}OH_3)(O_2C^tBu)_4(HO_2C^tBu)_4](Et_3NH)_2$	65	43.79 (43.88)	7.50 (7.37)	1.65 (1.65)	6.96 (6.91)	19.68 (19.44)
24	$[Ni^{II}_2Er^{III}_2(\mu\text{-}OH_3)(O_2C^tBu)_4(HO_2C^tBu)_4](Et_3NH)_2$	50	43.56 (43.75)	7.47 (7.34)	1.64 (1.65)	6.86 (6.90)	19.70 (19.66)
25	$[Cu^{II}_2Gd^{III}_2(\mu\text{-}OH_3)(O_2C^tBu)_4(HO_2C^tBu)_4](^iPr_2NH_2)_2$	47	43.59 (44.70)	7.31 (7.39)	3.21 (3.16)	7.16 (7.17)	17.98 (17.74)
26	$[Cu^{II}_2Dy^{III}_2(\mu\text{-}OH_3)(O_2C^tBu)_4(HO_2C^tBu)_4](^iPr_2NH_2)_2$	52	43.59 (44.44)	7.54 (7.34)	3.24 (3.14)	7.08 (7.12)	18.17 (18.22)
27	$[Cu^{II}_2Ho^{III}_2(\mu\text{-}OH_3)(O_2C^tBu)_4(HO_2C^tBu)_4](^iPr_2NH_2)_2$	38	43.89 (43.98)	7.18 (7.27)	2.30 (2.40)	7.15 (7.27)	18.71 (18.87)
28	$[Cu^{II}_2Er^{III}_2(\mu\text{-}OH_3)(O_2C^tBu)_4(HO_2C^tBu)_4](^iPr_2NH_2)_2$	51	43.87 (43.87)	7.17 (7.25)	2.38 (2.40)	7.24 (7.25)	18.99 (19.09)

a. Calculated based on Mg^{II} and transition metal pivalate

Table S2. Crystallographic information for Dy-containing molecules.

	3	**15**	**9**	**21**	**25**
chem formula	$Mg_2Dy_2N_2O_{22}C_{62}C_{124}$	$Mn_2Dy_2N_2O_{22}C_{62}C_{122}$	$Co_2Dy_2N_2O_{22}C_{62}C_{124}$	$Ni_2Dy_2N_2O_{22}C_{62}C_{124}$	$Cu_2Dy_2N_2O_{22}C_{62}C_{124}$
fw	1623.24	1871.72	1638.06	1692.04	1735.72
cryst system	monoclinic	triclinic	triclinic	monoclinic	triclinic
space group	*P21/c*	*P-1*	*P-1*	*C2/c*	*P-1*
a/Å	15.4531(3)	13.2219(2)	11.3913(4)	20.7072(4)	11.1732(4)
b/Å	19.5753(4)	13.5495(3)	13.3809(5)	21.2970(3)	13.2788(4)
c/Å	14.0907(3)	14.1560(2)	15.4188(5)	18.3086(3)	15.5030(6)
α/°	90	71.5364(15)	103.070(3)	90	102.315(3)
β/°	109.082(2)	64.2521(15)	98.378(3)	101.572(2)	97.228(3)
γ/°	90	81.4352(15)	109.653(3)	90	110.072(3)
V/Å^3	4028.20(15)	2166.49(7)	2092.04(14)	7910.0(2)	2060.48(14)
Z	2	1	1	4	1
ρ calcd/g cm^{-3}	1.338	1.435	1.300	1.421	1.399
T/K	150.06(15)	106(6)	104.2(2)		102(1)
μ (Mo Kα)/mm^{-1}	1.920	2.963	2.215	2.401	2.367
$R_1(I>2\sigma(I))$[a]	0.0347	0.0311	0.0318	0.0219	0.0303
wR_2[a]	0.0662	0.0888	0.0727	0.0515	0.0688

a $R_1 = \sum||F_o| - |F_c||/|F_o|$, $wR_2=[w(|F_o| - |F_c|)^2/w|F_o|^2]^{1/2}$

Table S3. Crystallographic information for Er-containing molecules.

	5	**17**	**11**	**23**	**27**
chem formula	$Mg_2Er_2N_2O_{22}C_{62}C_{124}$	$Mn_2Er_2N_2O_{22}C_{62}C_{122}$	$Co_2Er_2N_2O_{22}C_{62}C_{124}$	$Ni_2Er_2N_2O_{22}C_{62}C_{124}$	$Cu_2Er_2N_2O_{22}C_{62}C_{124}$
fw	1623.24	1871.72	1638.06	1692.04	1735.72
cryst system	monoclinic	triclinic	triclinic	monoclinic	triclinic
space group	*P21/c*	*P-1*	*P-1*	*C2/c*	*P-1*
a/Å	15.4531(3)	13.2219(2)	11.3913(4)	20.7072(4)	11.1732(4)
b/Å	19.5753(4)	13.5495(3)	13.3809(5)	21.2970(3)	13.2788(4)
c/Å	14.0907(3)	14.1560(2)	15.4188(5)	18.3086(3)	15.5030(6)
α/°	90	71.5364(15)	103.070(3)	90	102.315(3)
β/°	109.082(2)	64.2521(15)	98.378(3)	101.572(2)	97.228(3)
γ/°	90	81.4352(15)	109.653(3)	90	110.072(3)
V/Å^3	4028.20(15)	2166.49(7)	2092.04(14)	7910.0(2)	2060.48(14)
Z	2	1	1	4	1
ρ calcd/g cm^{-3}	1.338	1.435	1.300	1.421	1.399
T/K	150.06(15)	106(6)	104.2(2)		102(1)
μ (Mo Kα)/mm^{-1}	1.920	2.963	2.215	2.401	2.367
$R_1(I>2\sigma)(I))$[a]	0.0347	0.0311	0.0318	0.0219	0.0303
wR_2[a]	0.0662	0.0888	0.0727	0.0515	0.0688

a $R_1 = \sum||F_O| - |F_c||/|F_o|$, $wR_2=[w(|F_o| - |F_c|)^2/w|F_o|^2]^{1/2}$

Table S4. Unit Cells determination for remaining clusters

chem formula	**{Mg_2Y_2}**	**{Mg_2Tb_2}**	**{Mg_2Ho_2}**	**{Mn_2Tb_2}**	**{Mn_2Ho_2}**	**{Mn_2Er_2}**	**{Co_2Y_2}**
a/Å	12.9400(11)	15.7443(5)	15.4985(4)	16.8219(4)	16.8346(3)	13.2163(7)	11.3596(3)
b/Å	14.1629(12)	13.1628(4)	19.5983(5)	13.1584(2)	13.1278(3)	13.5584(5)	13.2938(4)
c/Å	14.2789(10)	21.9247(9)	14.1128(3)	21.4410(5)	21.5476(3)	14.1537(7)	15.4073(4)
α/°	98.793(7)	90	90	90	90	71.640(4)	102.961(3)
β/°	108.203(7)	109.812(4)	109.120(3)	109.994(3)	109.766(3)	64.229(5)	98.742(2)
γ/°	116.745(9)	90	90	90	90	81.467(4)	109.556(3)
V/Å^3	2082.94	4274.73	4050.2	4487.55	4481.47	2167.52	2070.26
chem formula	**{Co_2Tb_2}**	**{Co_2Ho_2}**	**{Co_2Er_2}**	**{Cu_2Ho_2}**	**{Cu_2Er_2}**	**{Ni_2Tb_2}**	**{Ni_2Ho_2}**
a/Å	15.7469(4)	15.8238(7)	10.5068(9)	11.2038(5)	11.2136(5)	15.9241(5)	20.7201(6)
b/Å	13.0245(3)	13.0747(4)	14.4090(12)	13.3226(6)	13.3202(6)	12.9928(3)	21.3022(5)
c/Å	21.9609(5)	22.0964(8)	14.7534(7)	15.5565(5)	15.5839(7)	21.7668(8)	18.2890(5)
α/°	90	90	77.808(7)	102.642(3)	102.470(4)	90	90

β/°	110.893(3)	110.860(4)	69.522(8)	96.869(3)	97.202(4)	111.049(4)	101.679(3)
γ/°	90	90	81.934(7)	110.014(4)	110.001(4)	90	90
V/Å^3	4207.91	4171.91	2039.83	2080.42	2084.77	4203.02	7905.75

Table S5. Continuous shaped measures (CShM) for $\{M_2Dy_2\}$ obtained using SHAPE.

	{Mg_2Dy_2}	**{Mn_2Dy_2}**	**{Co_2Dy_2}**	**{Ni_2Dy_2}**	**{Cu_2Dy_2}**
OP-8	32.114	32.1761	32.110	32.319	32.677
HPY-8	21.838	21.497	21.619	21.638	21.178
HBPY-8	17.782	17.561	17.468	17.486	16.784
CU-8	11.719	10.960	11.654	11.391	11.660
SAPR-8	2.323	1.973	2.270	2.114	2.280
TDD-8	2.811	2.773	2.621	2.996	2.363
JGBF-8	15.664	15.959	15.818	15.396	15.001
JETBPY-8	28.249	27.552	28.570	27.732	28.331
JBTPR-8	4.373	3.702	4.041	3.847	3.839
BTPR-8	3.094	2.641	2.801	2.745	2.669
JSD-8	5.853	5.726	5.561	5.742	5.101
TT-8	12.521	11.620	12.402	12.114	12.285
ETBPY-8	23.152	23.022	23.469	22.515	24.112

OP-8 = (D_{8h}) Octagon
HPY-8 = (C_{7v}) Heptagonal pyramid
HBPY-8 = (D_{6h}) Hexagonal bipyramid
CU-8 = (O_h) Cube
SAPR-8 = (D_{4d}) Square antiprism
TDD-8 = (D_{2d}) Triangular dodecahedron
JGBF-8 = (D_{2d}) Johnson gyrobifastigium J26
JETBPY-8 = (D_{3h}) Johnson elongated triangular bipyramid J14
JBTPR-8 = (C_{2v}) Biaugmented trigonal prism J50
BTPR-8 = (C_{2v}) Biaugmented trigonal pris
JSD-8 = (D_{2d}) Snub diphenoid J84
TT-8 = (T_d) Triakis tetrahedron
ETBPY-8 = (D_{3h}) Elongated trigonal bipyramid

Table S6. Magnetic data for clusters $\{M_2Ln_2\}$.

	Mg_2Gd_2	Mg_2Tb_2	Mg_2Dy_2	Mg_2Ho_2	Mn_2Er_2	Mn_2Y_2	Mn_2Gd_2
S ($M^{2+/3+}$)	-	-	-	-	-	2	2
S (Ln^{3+})	7/2	3	5	2	3/2	-	7/2
L (Ln^{3+})	0	3	5/2	6	6	-	0
J (Ln^{3+})	7/2	6	15/2	8	15/2	-	7/2
g_J (Ln^{3+})	1.99	3/2	4/3	5/4	6/5	-	1.99
g ($M^{2+/3+}$)	-	-	-	-	-	2.12	2.12
$\chi_M T$/ (calcd)[b]	15.59	23.62	28.33	28.12	22.95	6.74	22.33
$\chi_M T$ (obs)[a,b]	15.70	23.26	27.80	27.84	22.35	1.76	19.62
$\chi_M T$ (at 2K)[b]	15.32	4.31	28.65	14.60	17.06	0.07	15.30
M_β (obs at 1.8 K)[c]	13.74	9.53	10.78	10.19	9.67	0	13.97

S (total spin angular momentum), *L* (total orbital angular momentum) and *J* (total angular momentum), of the ground multiplet. g_J is the Landé factor. [a]Room temperature $\chi_M T$, [b]Values of $\chi_M T$ are given in emu mol^{-1} K, [c]Values of *M* are given in μ_B mol^{-1}, value observed at 7 T. [d]Magnetisation measured at 2 K and 7 T.

Table S6 continued. Magnetic data for clusters $\{M_2Ln_2\}$.

	Mn_2Tb_2	Mn_2Dy_2	Mn_2Ho_2	Mn_2Er_2	Co_2Y_2	Co_2Gd_2
S ($M^{2+/3+}$)	2	2	2	2	3/2	3/2
S (Ln^{3+})	3	5	2	3/2	-	7/2
L (Ln^{3+})	3	5/2	6	6	-	0
J (Ln^{3+})	6	15/2	8	15/2	-	7/2
g_J (Ln^{3+})	3/2	4/3	5/4	6/5	-	1.99
g ($M^{2+/3+}$)	2.12	2.12	2.12	2.12		
$\chi_M T$/ (calcd)[b]	30.36	35.07	34.86	29.69		
$\chi_M T$ (obs)[a,b]	25.81	29.68	30.03	24.9	5.59	21.8
$\chi_M T$ (at 2K)[b]	13.62	24.28	12.79	11.79	0.47	15.75
M_β (obs at 1.8 K)[c]	9.72	10.22	9.62	9.97	4.28[d]	17.76[d]

S (total spin angular momentum), *L* (total orbital angular momentum) and *J* (total angular momentum), of the ground multiplet. g_J is the Landé factor. [a]Room temperature $\chi_M T$, [b]Values of $\chi_M T$ are given in emu mol^{-1} K, [c]Values of *M* are given in μ_B mol^{-1}, value observed at 7 T. [d]Magnetisation measured at 2 K

Table S6 continued. Magnetic data for clusters $\{M_2Ln_2\}$.

	Co_2Tb_2	Co_2Dy_2	Co_2Ho_2	Co_2Er_2	Ni_2Y_2	Ni_2Gd_2	Ni_2Tb_2
S ($M^{2+/3+}$)	3/2	3/2	3/2	3/2	1	1	1
S (Ln^{3+})	3	5	2	3/2	-	7/2	3
L (Ln^{3+})	3	5/2	6	6	-	0	3
J (Ln^{3+})	6	15/2	8	15/2	-	7/2	6
g_J (Ln^{3+})	3/2	4/3	5/4	6/5	-	1.99	3/2
g ($M^{2+/3+}$)					2.34	2.34	2.34
$\chi_M T$/ (calcd)[b]					2.74	18.32	26.36
$\chi_M T$ (obs)[a,b]	29.09	33.39	33.43	28.60	2.62	18.39	26.76
$\chi_M T$ (at 2K)[b]	4.34	20.70	12.10	16.25	0.14	17.46	5.65
M_β (obs at 1.8 K)[c]	13.74	14.45	14.74	14.15	0.61[d]	15.12	9.28

S (total spin angular momentum), *L* (total orbital angular momentum) and *J* (total angular momentum), of the ground multiplet. g_J is the Landé factor. [a]Room temperature $\chi_M T$, [b]Values of $\chi_M T$ are given in emu mol^{-1} K, [c]Values of *M* are given in μ_B mol^{-1}, value observed at 7 T. [d]Magnetisation measured at 2 K and 7 T.

Table S6 continued. Magnetic data for clusters $\{M_2Ln_2\}$.

	Ni_2Dy_2	Ni_2Ho_2	Ni_2Er_2	Cu_2Gd_2	Cu_2Dy_2	Cu_2Ho_2	Cu_2Er_2
S ($M^{2+/3+}$)	1	1	1	1/2	1/2	1/2	1/2
S (Ln^{3+})	5	2	3/2	7/2	5	2	3/2
L (Ln^{3+})	5/2	6	6	0	5/2	6	6
J (Ln^{3+})	15/2	8	15/2	7/2	15/2	8	15/2
g_J (Ln^{3+})	4/3	5/4	6/5	1.99	4/3	5/4	6/5
g ($M^{2+/3+}$)	2.34	2.33	2.34	2.05	2.05	2.05	2.05
$\chi_M T$/ (calcd)[b]	31.07	30.86	25.69	16.38	29.11	28.90	23.74
$\chi_M T$ (obs)[a,b]	30.31	31.05	25.13	17.30	28.1	27.99	23.64
$\chi_M T$ (at 2K)[b]	23.69	10.07	17.59	15.40	20.62	7.37	11.39
M_β (obs at 1.8 K)[c]	10.47	11.08[d]	11.29	13.71	10.51[d]	10.00	10.36

S (total spin angular momentum), L (total orbital angular momentum) and J (total angular momentum), of the ground multiplet. g_J is the Landé factor. [a]Room temperature $\chi_M T$, [b]Values of $\chi_M T$ are given in emu mol^{-1} K, [c]Values of M are given in μ_B mol^{-1}, value observed at 7 T. [d]Magnetisation measured at 2 K

Table S7. CASSCF calculated magnetic states for $\{Mg_2Dy_2\}$

E (cm^{-1})	g_x	g_y	g_z	Angle (°)
0.0	0.01	0.01	19.76	-
119.1	0.02	0.03	17.85	23.5
239.5	0.12	0.35	13.97	24.1
308.1	1.42	3.33	16.32	89.3
348.4	4.21	4.97	7.97	57.0
387.5	0.02	1.25	12.24	50.0
480.8	0.67	0.72	16.34	68.4
745.7	0.02	0.03	19.74	82.6

Table S8. CASSCF calculated magnetic states for $\{Mn_2Dy_2\}$

E (cm^{-1})	g_x	g_y	g_z	Angle (°)
0.0	0.01	0.01	19.79	-
63.3	0.07	0.09	17.25	11.7
213.3	0.54	0.74	14.10	12.5
336.7	2.03	4.39	10.10	33.7
385.0	2.15	5.39	9.60	88.1

432.4	0.20	2.45	11.59	54.0
482.8	0.98	2.25	14.98	66.1
694.8	0.00	0.03	19.66	88.4

Table S9. CASSCF calculated magnetic states for $\{Co_2Dy_2\}$

E (cm^{-1})	g_x	g_y	g_z	Angle (°)
0.0	0.01	0.02	19.68	-
124.8	0.05	0.07	17.93	24.8
221.8	0.23	0.44	14.14	27.2
283.5	0.47	0.95	17.27	89.5
323.5	4.24	5.85	8.82	79.4
357.8	1.03	2.52	13.27	61.3
440.0	0.78	0.80	16.42	68.1
713.4	0.02	0.03	19.77	82.3

Table S10. CASSCF calculated magnetic states for $\{Ni_2Dy_2\}$

E (cm^{-1})	g_x	g_y	g_z	Angle (°)
0.0	0.01	0.02	19.60	-
140.9	0.03	0.05	17.83	23.4
219.2	0.38	0.96	14.51	32.2
262.0	0.37	1.92	17.54	82.7
297.9	3.06	4.75	12.26	53.6
336.0	0.88	3.18	11.99	58.5
407.1	0.93	1.86	15.81	67.4
689.4	0.01	0.02	19.79	81.9

Table S11. CASSCF calculated magnetic states for $\{Cu_2Dy_2\}$

E (cm^{-1})	g_x	g_y	g_z	Angle (°)
0.0	0.03	0.06	19.31	-
126.4	0.29	0.34	17.68	28.6
169.0	0.75	1.16	14.75	37.0
218.3	2.16	3.36	15.60	85.7
269.5	0.56	4.37	6.38	60.3
295.1	0.67	5.93	12.83	84.3
339.9	1.28	2.34	14.73	62.3
614.3	0.01	0.03	19.77	78.0

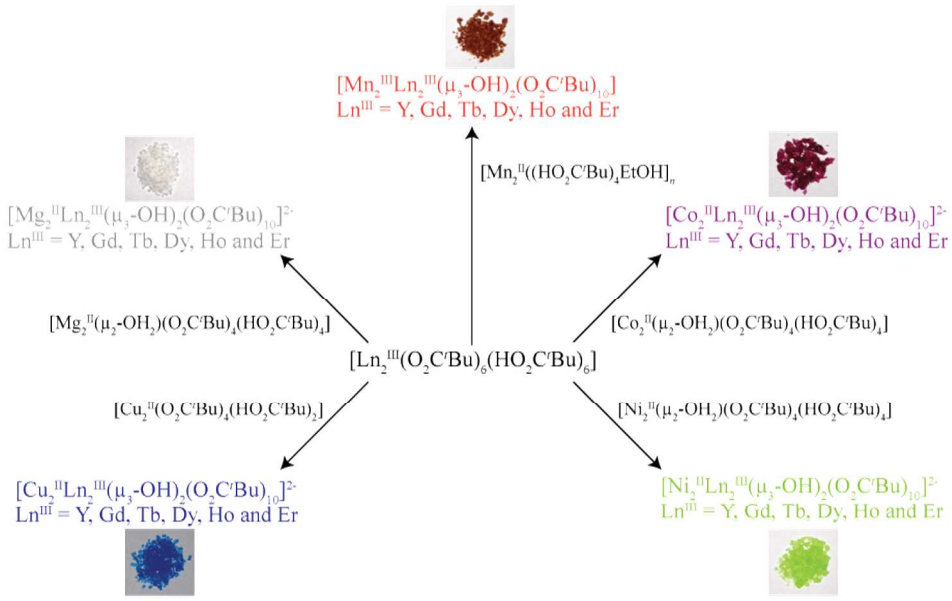

Scheme 1. Synthetic procedures and photos of crystals obtained.

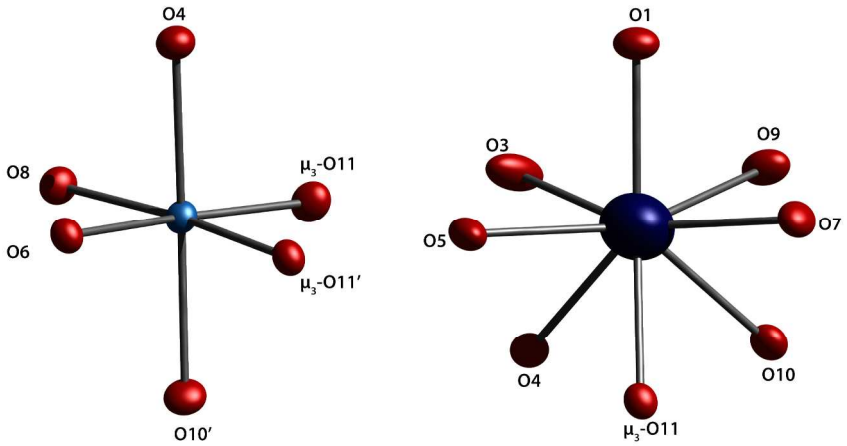

Figure S1. Geometry of 3d (left) and 4f (right) metals in the butterfly-like cluster. Colour code: Dy, blue; Mg, cyan; O, red; C, grey; H omitted for clarity.

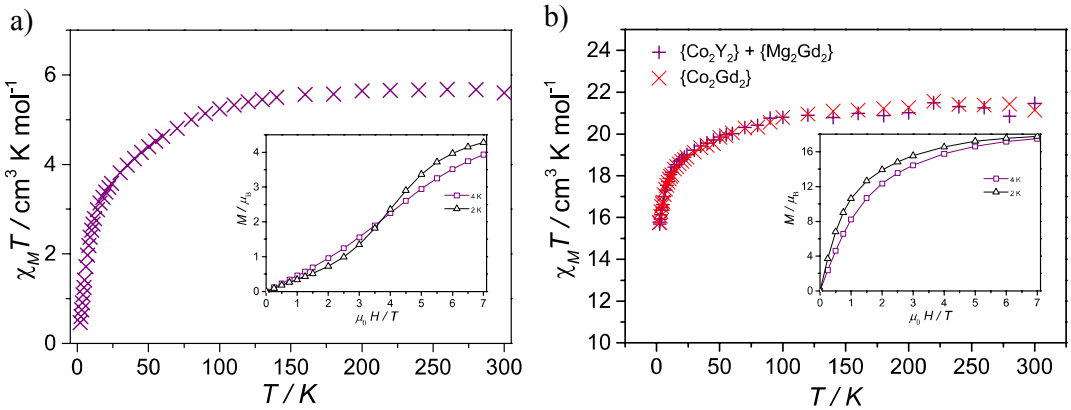

Figure S2. (a) Experimental $\chi_M T(T)$ and $M_\beta(H,T)$ (inset) data for $\{Co_2Y_2\}$; (b) experimental $\chi_M T(T)$ (purple symbols) and $M_\beta(H,T)$ (inset) data for $\{Co_2Gd_2\}$ [$\{Co_2Y_2\}$ + $\{Mg_2Gd_2\}$] (red symbols).

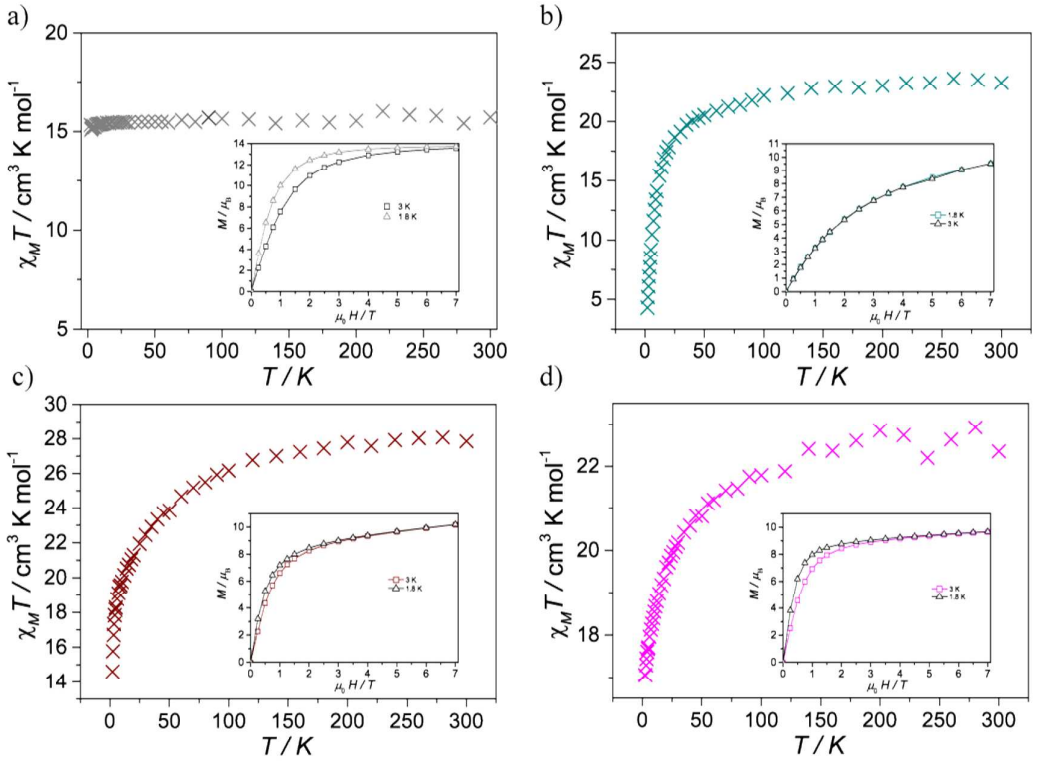

Figure S3. Experimental $\chi_M T(T)$ and $M_\beta(H,T)$ (inset) data for: (a) $\{Mg_2Gd_2\}$; (b) $\{Mg_2Tb_2\}$; (c) $\{Mg_2Ho_2\}$ and (d) $\{Mg_2Er_2\}$.

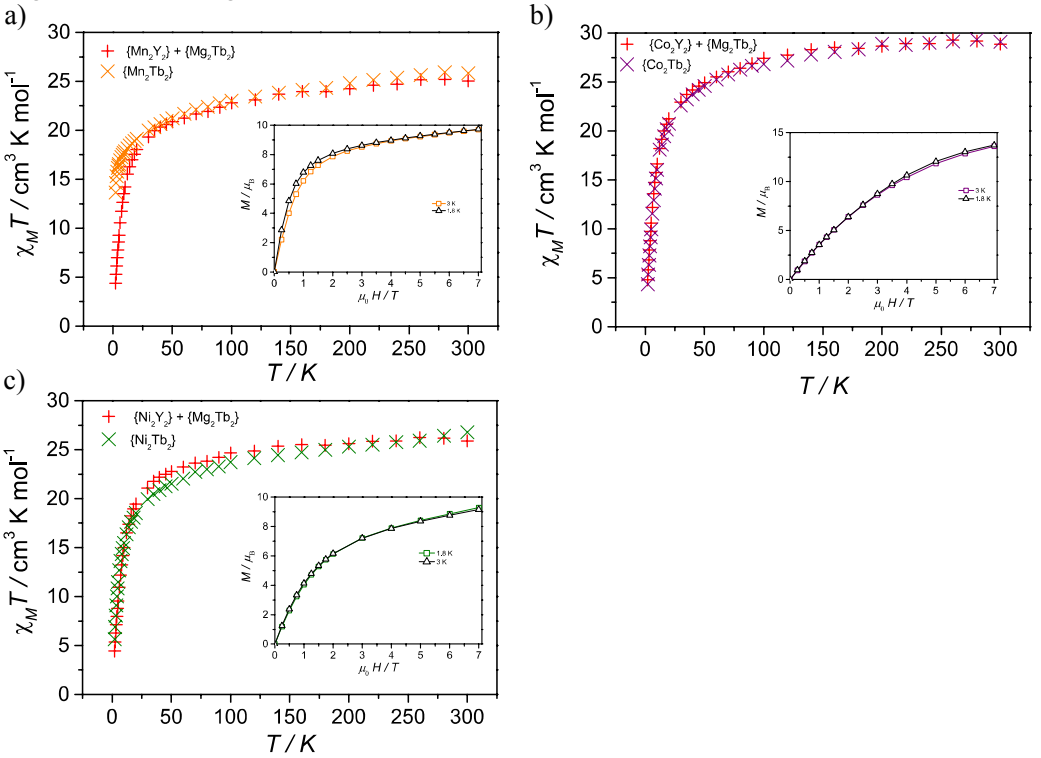

Figure S4. Comparison $\chi_M T(T)$ magnetic behaviour for $\{M_2Tb_2\}$ and $[\{M_2Y_2\} + \{Mg_2Tb_2\}]$ were M = Mn (a); Co (b) and Ni (c); inset is the $M_\beta(H,T)$ behaviour for the pure $\{M_2Tb_2\}$, where M = Mn (a); Co (b) and Ni (c)

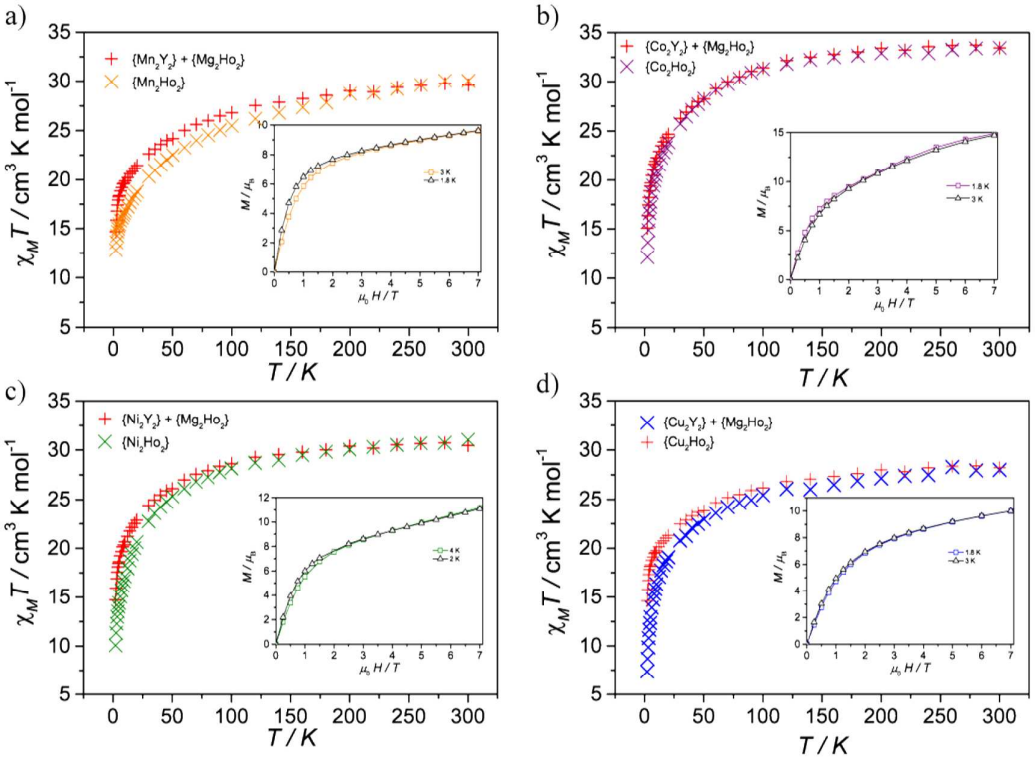

Figure S5. Comparison $\chi_M T(T)$ magnetic behaviour for $\{M_2Ho_2\}$ and $[\{M_2Y_2\} + \{Mg_2Ho_2\}]$ were M = Mn (a); Co (b); Ni (c) and Cu (d); inset is the $M_\beta(H,T)$ behaviour for the pure $\{M_2Ho_2\}$, where M = Mn (a); Co (b); Ni (c) and Cu (d).

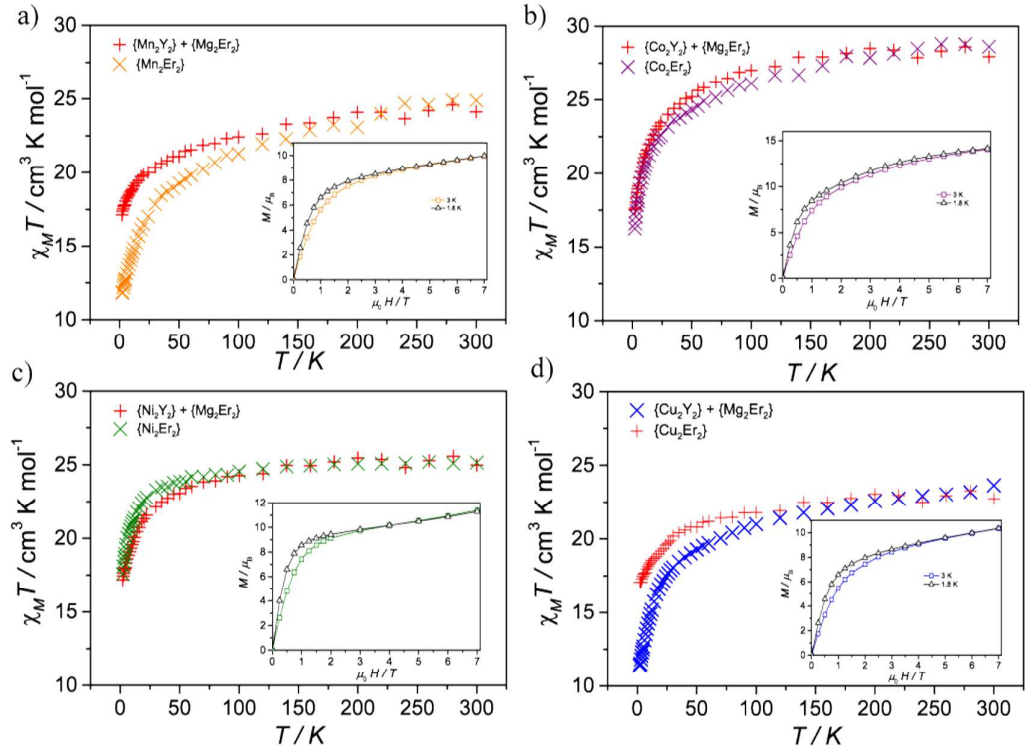

Figure S6. Comparison $\chi_M T(T)$ magnetic behaviour for $\{M_2Er_2\}$ and $[\{M_2Y_2\} + \{Mg_2Er_2\}]$ were M = Mn (a); Co (b); Ni (c) and Cu (d); inset is the $M_\beta(H,T)$ behaviour for the pure $\{M_2Er_2\}$, where M = Mn (a); Co (b); Ni (c) and Cu (d).

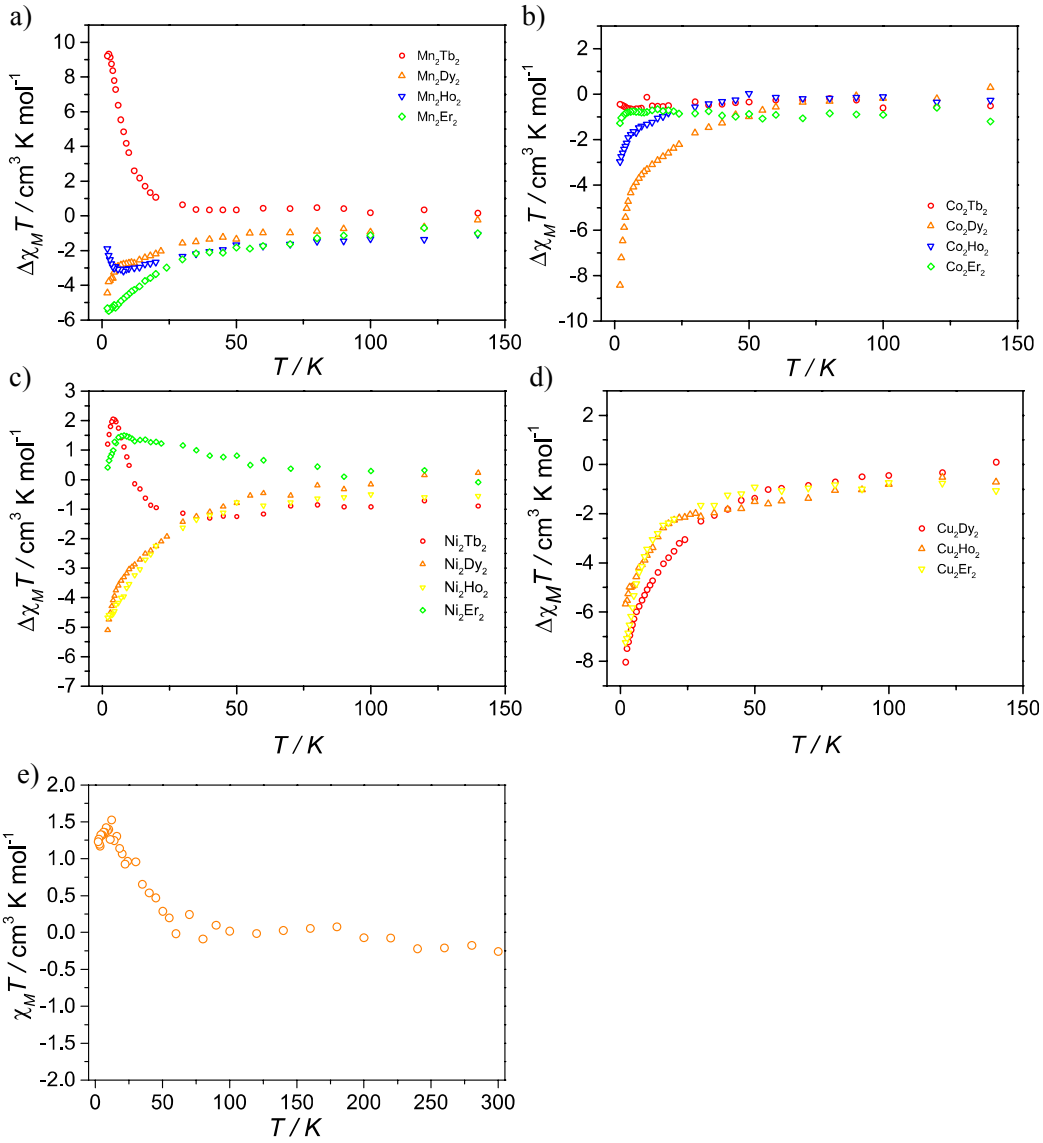

Figure S7. Comparison of magnetic behaviour using the $\Delta\chi_M T$ function of $\{M_2Ln_2\}$ – ($\{M_2Y_2\}$ + $\{Mg_2Ln_2\}$) were Ln = Tb, Dy, Ho and Er and M = Mn (a); Co (b); Ni (c) and Cu (d) and $\Delta\chi_M T$ function of $\{Mn_2Gd_2\}$ – ($\{Mn_2Y_2\}$ + $\{Mg_2Gd_2\}$ (e).

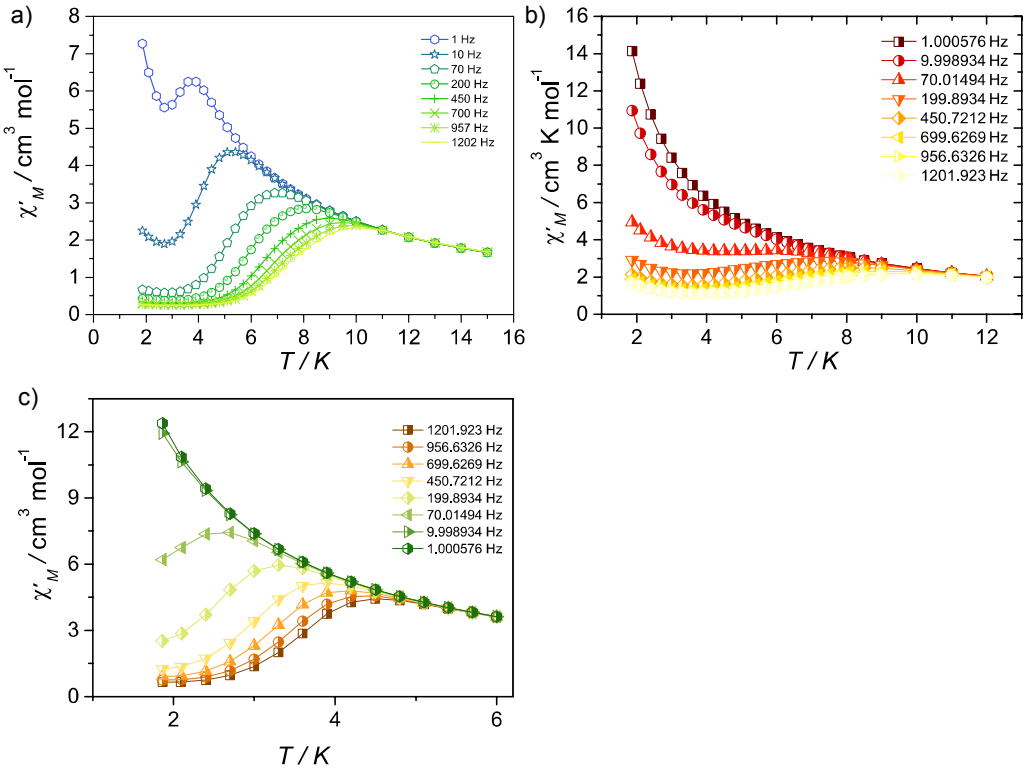

Figure S8. $\chi'_M(T)$ for: (a) $\{Mg_2Dy_2\}$; (b) $\{Mn_2Dy_2\}$; (c) $\{Ni_2Dy_2\}$.

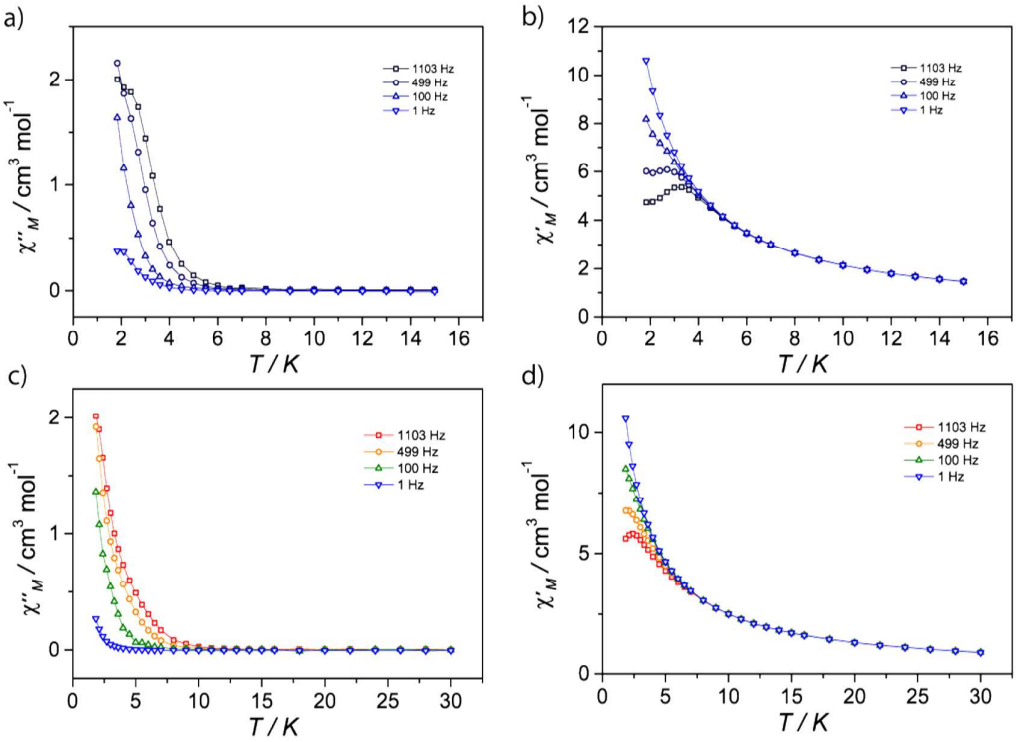

Figure S9. Temperature-dependence $\chi''_M(T)$ (a) and Frequency-dependence $\chi'_M(T)$ (b) for $\{Cu_2Dy_2\}$; Temperature-dependence $\chi''_M(T)$ (c) and Frequency-dependence $\chi'_M(T)$ (d) for $\{Co_2Dy_2\}$.

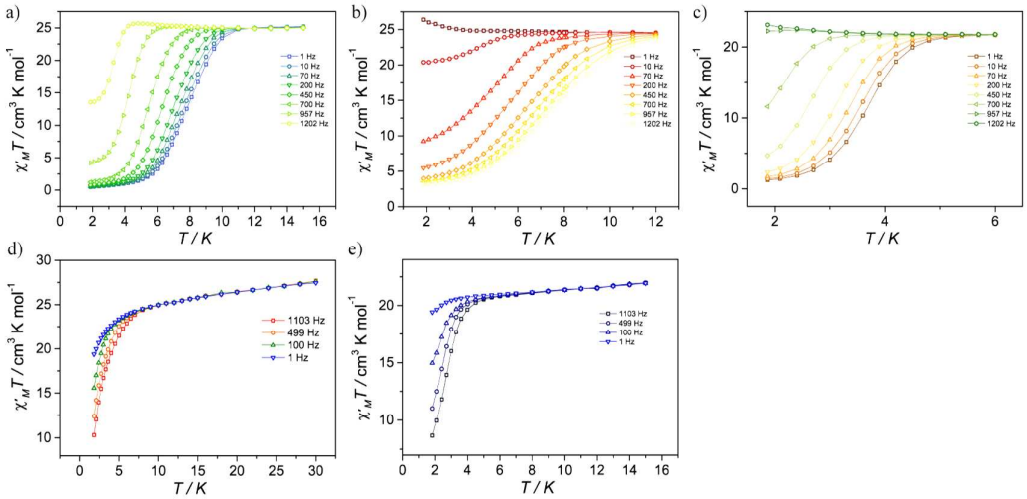

Figure S10. $\chi'_M T(T)$ for: (a) $\{Mg_2Dy_2\}$; (b) $\{Mn_2Dy_2\}$; (c) $\{Ni_2Dy_2\}$; (d) $\{Co_2Dy_2\}$; and (e) $\{Cu_2Dy_2\}$.